I J C T A, 9(37) 2016, pp. 725-735

Design and C-Leg Analysis of Leg Wheel Hybrid Hexapod Bot

M. Harikrishnan[*], K. Abbhivignesh[**], B. Karthikeyan[***] and M. Vignesh[****]

Abstract: The conventional mobile robotic platforms which either uses wheels or legs are quite familiar and each one of them has its own advantages and disadvantages. The wheeled robot is suitable for only plain and smooth terrain, whereas the legged robot can travel in any kind of terrain but is comparatively slower than the wheeled robot. So, a hybrid of both wheeled and legged platform would be quite suitable for any kind of terrain. The primary focus of this paper is to design and develop a leg-wheel hybrid robotic platform with a concurrent engineering and mechatronics approach to produce results with optimised design metrics at each and every stage of its development. An overall view of the entire mechatronics system is considered for design and development of the robot at each and every stage rather than a sequential engineering approach. This paper details the Finite Element Analysis (FEA) of the C – Legs which are used in the robot.

Index Terms: All terrain, analysis, hexapod, leg, machine learning, mobile robot, wheeled robot.

1. INTRODUCTION

Mobile robots are becoming quite essential now a days, as a deliberate need of robots has occurred in the field of exploration and surveillance in unknown terrain and environment. So, various advancement in locomotive mechanisms are continuously being researched and developed all over the world which would suit all the needs and make the robot quite adaptable to the unknown environment. One such advanced locomotive mechanism called the leg-wheel hybrid mechanism where the bot uses a hybrid of both leg like rotating C-Curves and wheels for locomotion. Furthermore, the suitable actuators that are used in the bot along with the programming implementation procedure has also been described in this paper.

This entire paper is structured as follows, section I covers the basic design specification of the bot, section, section III describes about the C-Leg bending calculations and material selection, section IV mentions the details of the actuators, electronics and programming platform used, section V explains the machine learning algorithm implementation and programming procedure, section VI explains the C-Leg analysis of the bot and the section VII is the conclusion of this research work and the future work to be done.

2. BASIC DESIGN SPECIFICATION OF THE BOT

Even though the leg-wheel hybrid mechanism in which the C-Leg used by the bot can be transformed into a wheel like structure is quite familiar and common [1], it has got lot of disadvantages like the transformation time in between the C-Leg and the wheel is quite high and not always reliable. The complexity in constructing such a mechanism is also very high and robustness of the system also reduces. So, considering all these facts, a simple and reliable design is developed for this bot as shown in Figure 1 and Figure 2. In this design the bottom panel of the bot holds the wheels, which will come in contact to the ground when all the legs are lifted up at once.

[*] Department of Mechatronics, SRM University. *Email: hari_madhusudhanan@srmuniv.edu.in*
[**] Department of Mechatronics, SRM University. *Email: aryan.technikart@gmail.com*
[***] Department of Mechatronics, SRM University. *Email: k6thi.27@gmail.com*
[****] Department of Mechatronics, SRM University. *Email: vignesh_manimaran@gmail.com*

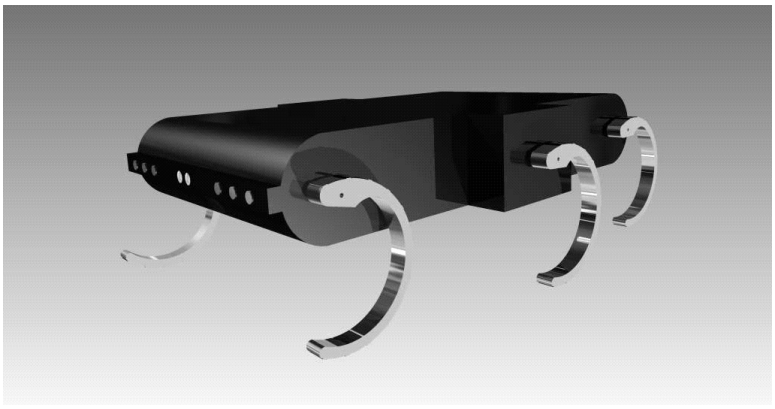

Figure 1: Basic design outlook of the bot in standing position using its C-Legs

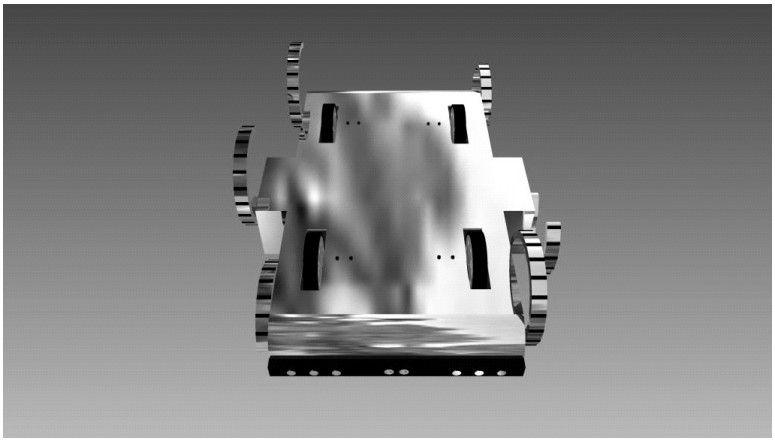

Figure 2: Bottom panel of the bot with its four wheels attached

The six C-Legs which are used in the bot gives it a good grip and stable walking position without much disturbances for the components inside the bot. The entire body of the body is made up of aluminium and the C-Legs are constructed using Manganese Steel. The detailed analysis of the C-Leg is described in the next section [7]. The bot moves using its C-Legs in uneven and difficult terrains in which the speed of movement will not be a main concern. In all other cases the bot would use its wheels for its locomotion. Compactness and robustness were the two main parameters which were considered while designing this bot. The actual image of the bot is as shown in the Figure 3. The sensors which are required are housed both in the front and the rear ends of the bot [8].

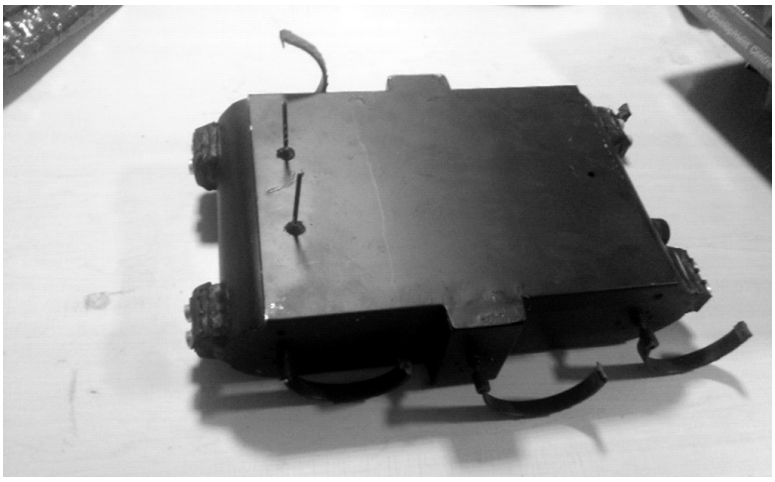

Figure 3: The actual image of the leg-wheel hybrid hexapod

3. C-LEG ANALYSIS

This section is primarily concentrated with the material selection and analysis of the C-Leg used in the bot. The material with which the C-Leg is made is this case is Manganese Steel. The general properties of Manganese Steel are listed as shown in Table 1.

Table 1
Mechanical Properties and Physical Properties of Manganese Steel

Mechanical properties	Hardness HB	Yield Strength MPa	UTS MPa	El%	KCV 20°C (68°F) – J
	220	380 (55 KSI)	940 (136 KSI)	40	≥ 112 J (≥ 83 ft.lbs)
Physical properties	Density	Expansion Coeff. 0 – 600°C	Specific Heat	Electrical Resistivity	Thermal Conductivity
	7.88	10^{-6} °C $^{-1}$ 21.5	J/Metric Kg. °C 502	μΩ.m 75	W/m. °C 13
		10^{-6} °F $^{-1}$ 11.9	BTU/lb°F .12	μΩ.m 75	BTU/hr.ft°F 7.3

While in motion when these C-Legs are subjected to load, even though there is deflection behaviour seen in these compliant legs, its magnitude and orientation is quite difficult to be calculated as there are quite a lot parameters to be considered which is mostly dependent upon the environment and the grips used for the C-Legs.

There are actually two models to analyse the C-Leg bending mechanisms, Pseudo Rigid Body (PRB) Model and Topology Optimisation.

In this case PRB model is used for bending analysis because the Topology Optimisation model requires specific boundary conditions for a given design space. Also, in PRB model, the leg stiffness can be easily calculated for different configurations and dimensions easily.

So in this PRB model, the point of deflection is first found out and a pivot point is set, from where the actual bending starts as shown in the Figure 4.

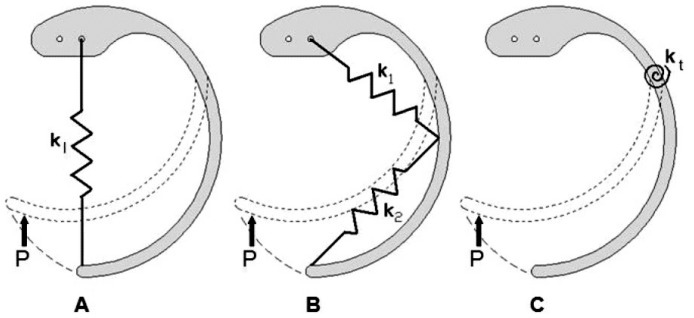

Figure 4: Determining the location of pivot point for bending in the C-Leg based on the spring stiffness k_1 and k_2 when being subjected to a load P

The stiffness factor of the material used for the leg is calculated (in this case 'manganese steel') with respect to the total weight of the bot (approx. 15 Kgs), where F is the force applied on the body and δ is the displacement due to bending.

$$k = \frac{F}{\delta} \tag{1}$$

The actual loading point does not occur in the tip of the complaint leg, because once the load is given the leg bends with an angle, which is the PRB angle (this angle is based on the overall load of the bot or the load acting on individual legs) and rests at a point called the loading point. The pseudo rigid body link is the measure from the pivot point and the loading point. The PRB angle is found with respect to the PRB link. The flexible region starts from the pivot to the loading point where the stiffness factor is considered to be less.So, the entire overview of all the legs with load acting visualisation is as shown in the Figure 5.

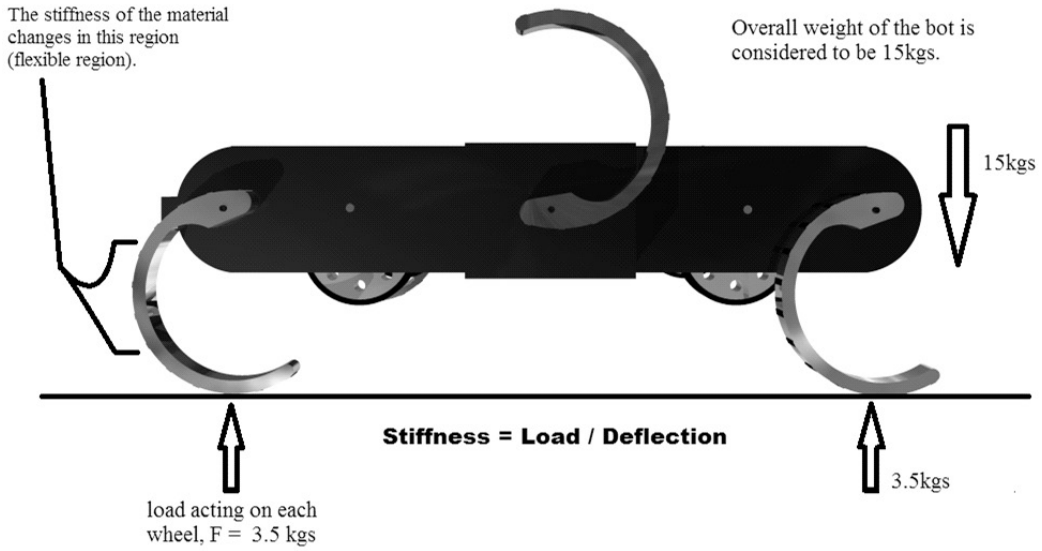

Figure 5: The flexible region and the load acting on individual leg while the bot is in running position is as depicted

Load acting on each leg is 3.5 kgs, because there are only four complaint legs which are in contact with the surface and also the load is considered to be distributed uniformly to each leg. The initial curvature and the length of the PRB link are ralated a non dimentioanalised parameter, k_o, which is also the leg arc length measured along axial point/initial radius, so, $k_o = l/R_i$. The PRB link length 'λ' is apporximately equal to the k_o. So the 'λ' value changes according to loading conditions (as the radius changes the 'λ' value is also changed). The PRB angle 'α' specifies the initial angle of the PRB link and 'β' is the actual angle of the PRB link with respect to the point of deflection or the pivot point. The tortional leg stiffness and the lateral leg stiffness define the design flexibility of the complaint legs.

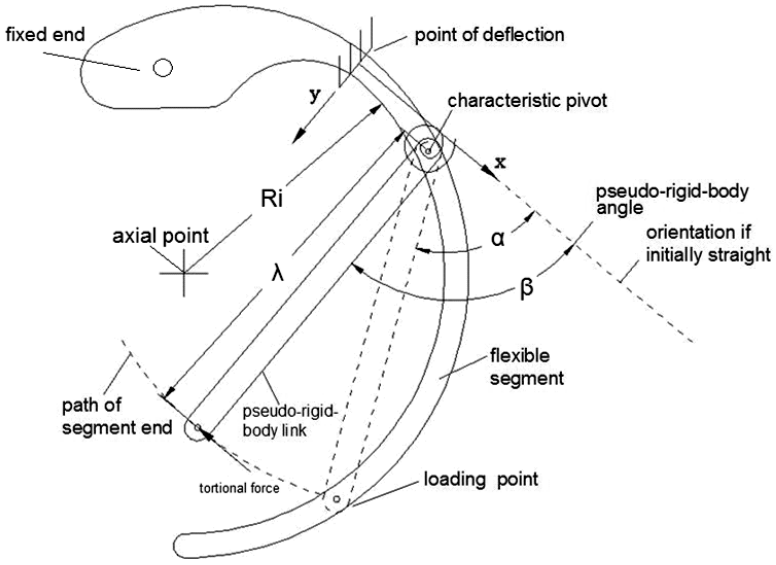

Figure 6: Determining the characteristic pivot, axial point and the flexible segment of the C-Leg bent structure

The tortional leg stiffness is given by,

$$K_t = \lambda K_\beta E I_s / l \quad (2)$$

Where E is the Young's modulus, I_s is the moment of inertia in the sagittal plane, l is the leg arc length and K_β is the stiffness coefficient. For initially straight beams K_β is a function of the angle at which the load is applied and for initially curved beams and k_o values near 1.0 and higher, K_β is relatively constant for tangential and compressive beam loading. Therefore, E, I_s, R_i, and l are the factors that is needed to approximate K_t in the PRB model.

The leg stiffness is characterised by the standard cantiliver beam bending equation,

$$K_L = 3EI_L / L^3 \quad (3)$$

Where I_L is the moment of inertia in the lateral direction, L is the linear distance from the point of deflection to the loading point. It is important to note that K_t and K_L can be independently specificed by changing the moment of inertia. This feature increases design flexibility and allows one to adjust spatial compliance in the lateral direction independent of the sagittal plane.

A linear guide is used for experimenting the stiffness of the complaint leg. The results are depicted in the Figure 7, where, tortional stiffness and the lateral stiffness are ploted with respect to the slider position [10].

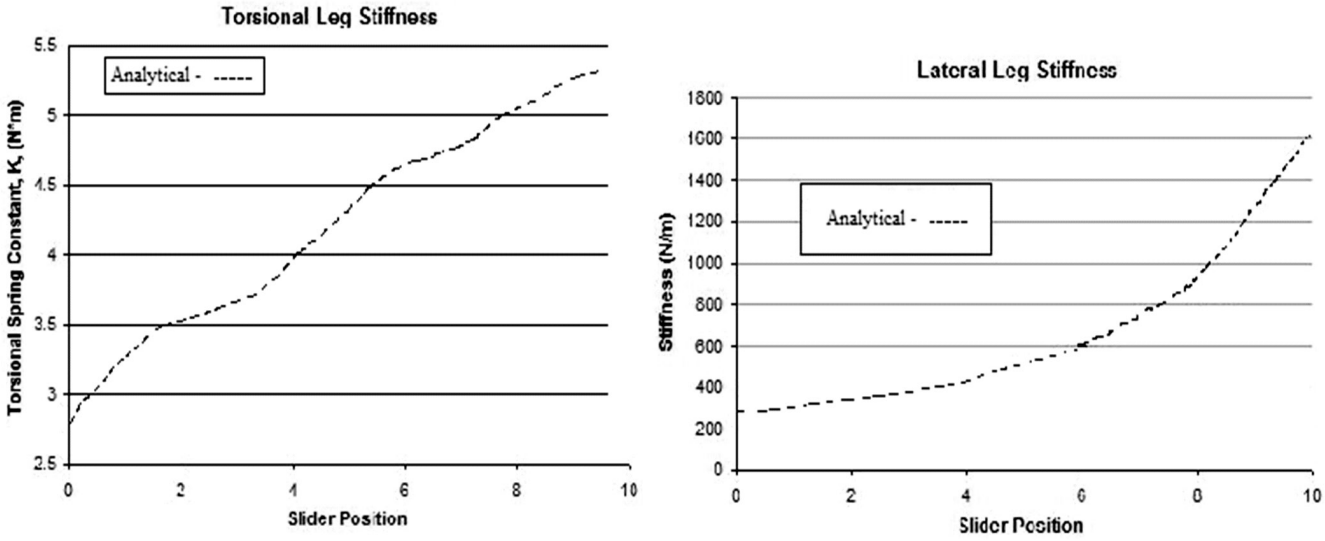

Figure 7: Torsional Stiffness and Lateral Stiffness of C-Leg of the bot is plotted in this graph with respect to the slider position

4. ACTUATORS, ELECTRONICS AND PROGRAMMING PLATFORM

The C-leg part of the bot is connected to the Dynamixel-MX-64T servo motors and the wheels are connected to the normal DC geared motors. There are many important reasons why these Dynamixels are quite suitable for this bot, which are listed as follows. First of all these motors use TTL connection logic which makes the connections between different motors quite simple. They have high precision, accuracy and also has good torque characteristics [3]. Most important of all, the machine learning algorithm implementation can be done quite easily using this servo motor as it has reliable and accurate feedbacks [12].

The main processor on board is the Raspberry Pi version 2, which is interconnected with various other sensor modules and the motor driver circuits. The overall layout of the entire electrical and electronics systems are as depicted in the Figure 8. The entire programming is done using the Linux based Robotic Operating System (ROS) and simulated using Gazebo [15].

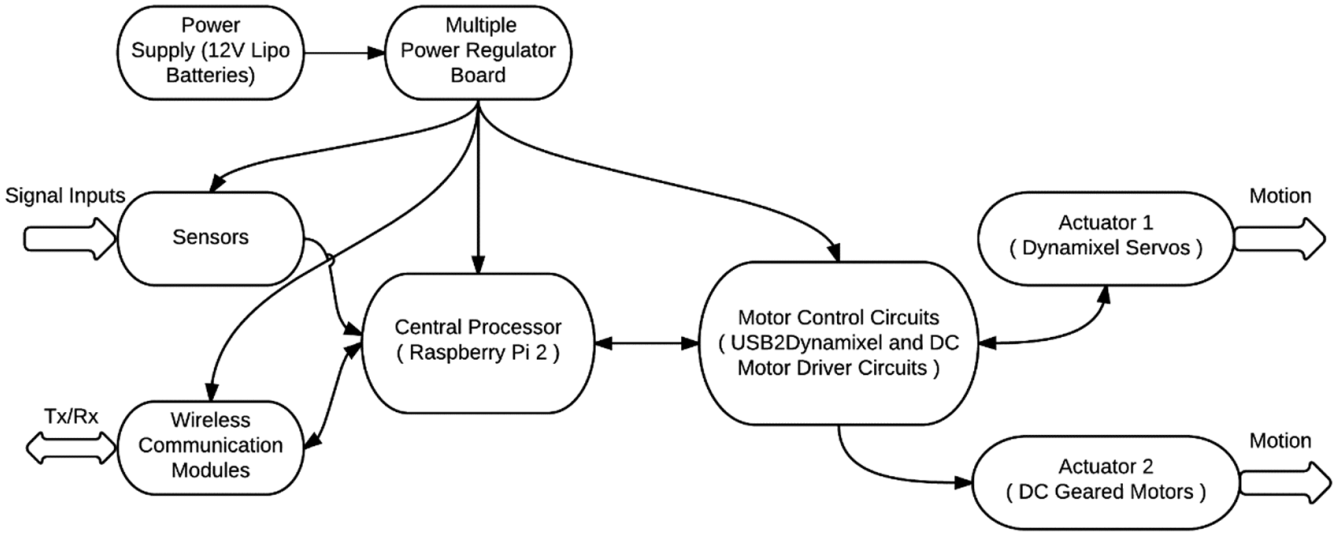

Figure 8: The above layout depicts the connection procedure in between various electrical and electronic components of the bot

The primary function of the sensor used is to identify the obstacle ahead of it and to determine its height. However the details regarding operational procedures of the sensors and the data acquisition are not covered in this paper as they are presented as a separate research work and henceforth in this paper the machine learning algorithm and programming implementation will be described.

5. MACHINE LEARNING ALGORITHM IMPLEMENTATION FOR OBSTACLE CROSSING

Even though all the actuators of the bot can be controlled manually, the main scope of this project is to introduce the concept of semi-automation through machine learning process which is detailed as follows. Whenever the bot bumps onto any non-crossable obstacle during forward motion, certain critical sequence of steps has to be taken by the bot to cross the obstacle, which is based on the height and width of the obstacle. So, the main aim is to implement an algorithm such that the bot would record these various operator controlled actuator movements done during the unknown obstacle crossing procedure based on certain height and width of the object [4]. So, whenever the bot detects a similar obstacle of same height and length, the operator need not repeat the same set of sequence, as the bot already knows which sub algorithm has to be carried out for crossing it from the stored values and repeats it.

The program implementation sequence for the above said problem statement is as shown in Figure 8.

The explanation for the flowchart shown in Figure 5 is as follows. Initially, when the bot is powered on, by default it is in semi-autonomous mode. I first scans for the presence of any user given input for movement. If any input is present it executed the corresponding algorithm for movement. If not, the previous movement algorithm is followed. After execution of the first movement algorithm it scans for the presence of any obstacle present ahead of it which is beyond its crossing capability with respect to the obstacles height and width. This process is done by using a standard image processing procedure [17]. If any such obstacle is present, the bot halts its movement and finds a suitable crossing algorithm for the corresponding height and width of the obstacle in its database. If no such match is found, the bot automatically switches to complete manual mode and waits for the user input for its motion [18]. The user input values to the motors are continuously stored in its database against the corresponding obstacle height and width. After the crossing by manual method is complete, the bot again switches back to the semi-autonomous mode and begins the next loop of operation once again [21]. So, this programming procedure makes sure that whenever the bot detects the presence of any similar obstacle once again, it automatically executes the algorithm from its database for crossing it successfully.

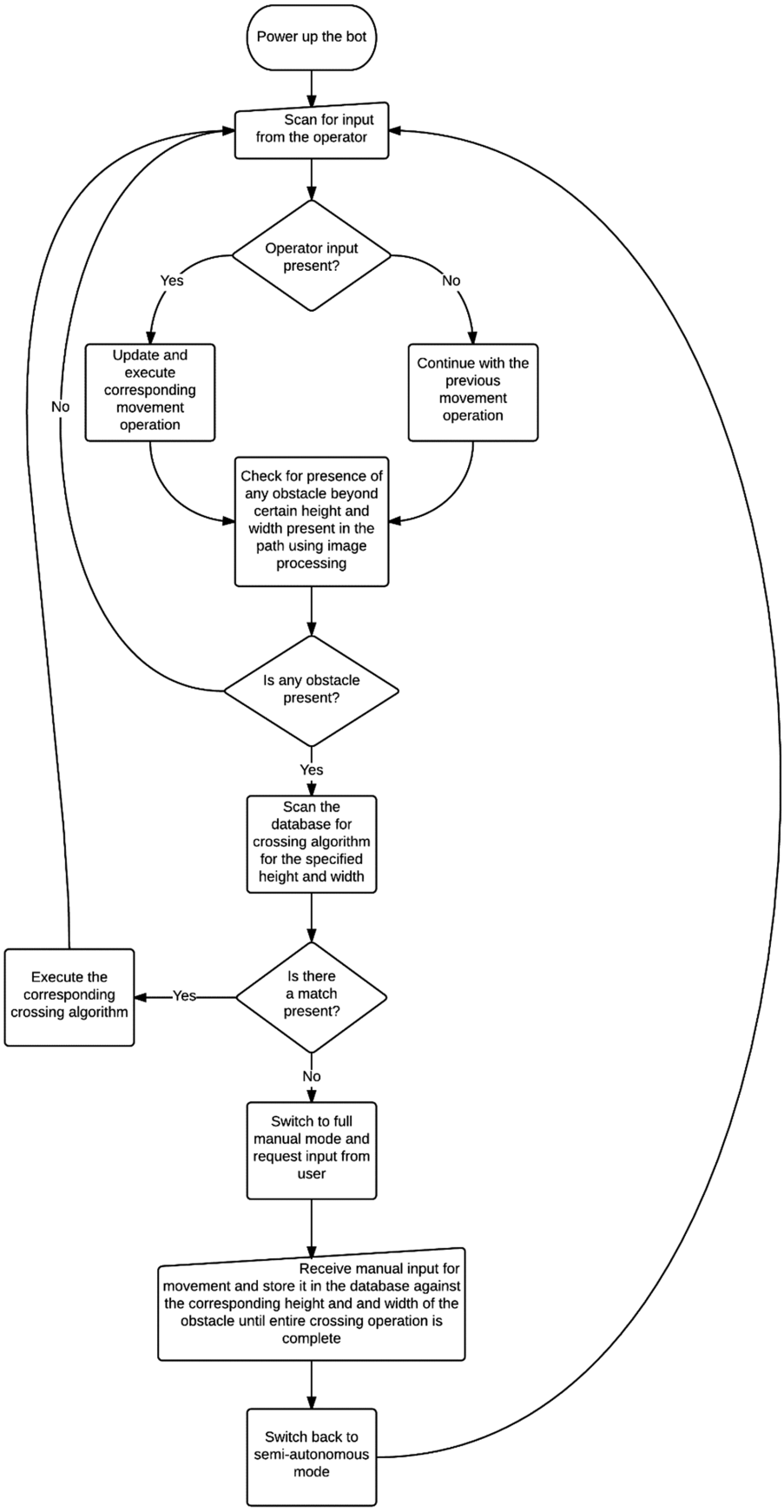

Figure 8: The flowchart represents the operation of the bot in semi-autonomous mode in which machine learning algorithm has been implemented for obstacle crossing procedure

6. FEA OF C - LEG

This section is primarily concentrated with the material selection and analysis of the C-Leg used in the bot. The details regarding the material selection for the C-Leg is as shown in Table 2.

Table 2
Material Specification of C-Leg

Name	*Aluminum 6061*	
General	Mass Density	2.7 g/cm^3
	Yield Strength	275 MPa
	Ultimate Tensile Strength	310 MPa
Stress	Young's Modulus	68.9 GPa
	Poisson's Ratio	0.33 ul
	Shear Modulus	25.9023 GPa
Part Name(s)	LEG	

After the material selection procedure, the mesh settings is done as shown in the Table 3.

Table 3
Mesh Settings for FEA

Avg. Element Size (fraction of model diameter)	0.005
Min. Element Size (fraction of avg. size)	0.01
Grading Factor	1.5
Max. Turn Angle	60 deg
Create Curved Mesh Elements	Yes

For instance, only one C-Leg out of six is taken into consideration as shown in the Figure 9, and analysed.

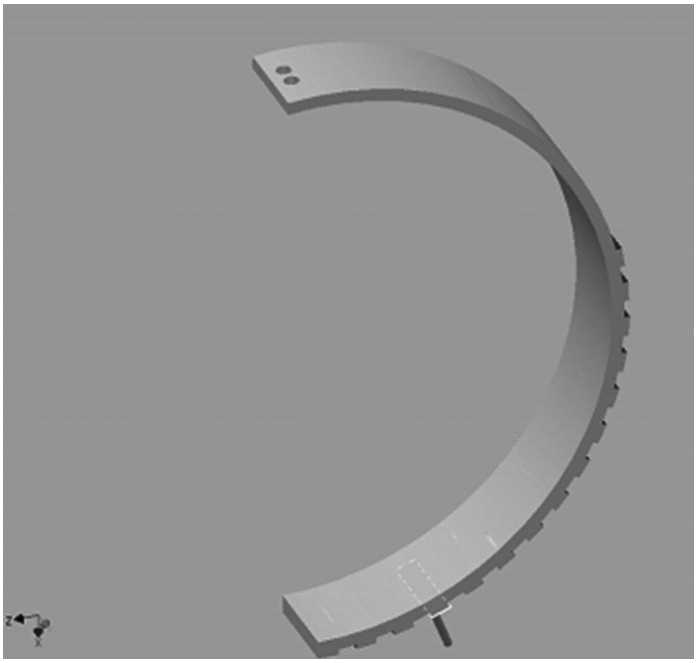

Figure 9: Unit C-Leg of Hexapod

In order to make the calculations simpler, a predefined constrain is fixed and the primary for specification is made according to the Table 4.

Table 4
Force Specifications

Load Type	*Force*
Magnitude	10.000 N
Vector X	–9.309 N
Vector Y	0.000 N
Vector Z	3.653 N

So, after the material selection, mesh settings, force and constrain definition, the FEA on C – Leg is done and the results are obtained as follows. The Table 5, represents the reaction for and moment on the defined constraints and the Table 6, depicts the entire result of the FEA process done.

Table 5
Reaction Force and Reaction Moment on Constraints

Constraint Name	*Reaction Force*		*Reaction Moment*	
	Magnitude	*Component (X,Y,Z)*	*Magnitude*	*Component (X,Y,Z)*
Fixed Constraint: 1	10 N	9.30874 N 0 N –3.65341 N	0.163141 N m	0 N m 0.163141 N m 0 N m

Table 6
FEA Complete Result

Name	*Minimum*	*Maximum*
Volume	9699.56 mm^3	
Mass	0.0261888 kg	
Von Mises Stress	0.00342306 MPa	50.9313 MPa
1st Principal Stress	–11.1816 MPa	62.5941 MPa
3rd Principal Stress	–37.8314 MPa	18.7251 MPa
Displacement	0 mm	3.21907 mm
Safety Factor	5.39943 ul	15 ul
Stress XX	–31.2069 MPa	58.777 MPa
Stress XY	–6.78295 MPa	6.45903 MPa
Stress XZ	–21.3637 MPa	17.6197 MPa
Stress YY	–16.2938 MPa	21.8471 MPa
Stress YZ	–7.15734 MPa	6.77936 MPa
Stress ZZ	–32.653 MPa	39.0959 MPa
X Displacement	–1.53503 mm	0.529129 mm
Y Displacement	–0.00118438 mm	0.00118522 mm
Z Displacement	–0.00135727 mm	2.8295 mm
Equivalent Strain	0.0000000831891 ul	0.000678095 ul
1st Principal Strain	–0.000000049409 ul	0.000775757 ul
3rd Principal Strain	–0.000460967 ul	0.0000000922365 ul
Strain XX	–0.000430334 ul	0.00076541 ul
Strain XY	–0.000130934 ul	0.000124681 ul
Strain XZ	–0.000412391 ul	0.000340118 ul
Strain YY	–0.00018817 ul	0.000139202 ul
Strain YZ	–0.000138161 ul	0.000130864 ul
Strain ZZ	–0.000318095 ul	0.00037109 ul

7. CONCLUSION AND FUTURE WORK

This paper is concentrated only with the basic design outlook, C-Leg material selection and bending analysis, basic electronics outlook and partial machine learning algorithm. The analysis of the different movements which are possible using the bot, complete electronics implementation, optimization of design metrics and implementation of complete machine learning procedure will be further researched in the future. Also, the possibility of underwater surveillance using this bot will all be researched. Furthermore, the stress-strain analysis across the bot when it is subjected to various movements and load distributions also will be studied in the future.

References

1. F. Michaud and S. Caron, "*Multi-modal locomotion robotic platform using leg-track wheel articulations*," Autonomous Robots, pp. 137–156, 2005.
2. J. Yuan and S. Hirose, "*Research on leg-wheel hybrid stairclimbing robot,zero carrier*," in IEEE International Conference on Robotics and Biomimetics, Vol. 1, 2004, pp. 654–659.
3. V. Krovi and V. Kumar, "*Modeling and control of a hybrid locomotion system*," ASME Journal of Mechanical Design, Vol. 121, No. 3, pp. 448–455, 1999.
4. S. D. Herbert, et al., "*Loper: A Quadruped-Hybrid Stair Climbing Robot*," in IEEE International Conference on Robotics and Automation (ICRA), 2008, pp. 799-804.
5. J. B. Jeans and D. Hong, "*IMPASS: Intelligent Mobility Platform with Active Spoke System*," in IEEE International Conference on Robotics and Automation (ICRA), 2009, pp. 1605 – 1606.
6. J. Y. Wong, Theory of Ground Vehicles: John Wiley and Sons Inc., 1993.
7. U. Saranli, et al., "*RHex: A simple and highly mobile hexapod robot*," International Journal of Robotics Research, Vol. 20, pp. 616-631, Jul 2001.
8. S.-Y. Shen, et al., "*Design of a Leg-Wheel Hybrid Mobile Platform*," in IEEE/RSJ International Conference on Intelligent Robots and Systems, 2009, pp. 4682-4687.
9. R. D. Quinn, et al., "*Parallel complementary strategies for implementing biological principles into mobile robots*," International Journal of Robotics Research, Vol. 22, pp. 169 186, 2003.
10. M. Guamieri, P. Debenesr, T. Inoh, E. Fukushima, and S. Hirose, "*Development of helios vii: an arm-equipped tracked vehicle for search and rescue operations*," in IEEE/RSJ International Conference on Intelligent Robots and Systems, 2004, pp. 39–45.
11. P. Liljeback, K. Y. Pettersen, O. Stavdahl, and J. T. Gravdahl, "*Snake robot locomotion in environments with obstacles*," IEEE/ASME Trans. Mechatronics, Vol. 17, No. 6, pp. 1158–1169, Dec. 2012.
12. N. O. Perez-Arancibia, J. P. Whitney, and R. J. Wood, "*Lift force control of flapping wing microrobots using adaptive feedforward schemes*," IEEE/ASME Trans. Mechatron., Vol. 18, No. 1, pp. 155–168, Feb. 2013.
13. S.Lohmeier,T.Buschmann, andH.Ulbrich, "*System design and control of anthropomorphic walking robot LOLA*," IEEE/ASME Trans. Mechatron., Vol. 14, No. 6, pp. 658–666, Dec. 2009.
14. Y. D. Hong and J. H. Kim, "*3-D command state-based modifiable bipedal walking on uneven terrain*," IEEE/ASME Trans. Mechatron., Vol. 18, No. 2, pp. 657–663, Apr. 2013.
15. D. J. Braun, J. E. Mitchell, and M. Goldfarb, "*Actuated dynamic walking in a seven-link biped robot*," IEEE/ASME Trans. Mechatron., Vol. 17, No. 1, pp. 147–156, Feb. 2012.
16. T. Seo and M. Sitti, "*Tank-likemodule-based climbing robot using passive compliant joints*," IEEE/ASME Trans.Mechatron., Vol. 18, No. 1, pp. 397– 408, Feb. 2012.
17. W. Hu, D. Marhefka, and D. E. Orin, "*Hybrid kinematic and dynamic simulation of running machines*," IEEE Trans. Robot., Vol. 21, No. 3, pp. 490–497, Jun. 2005.
18. J. T. Watson, R. E. Ritzmann, S. N. Zill, and A. J. Pollack, "*Control of obstacle climbing in the cockroach, Blaberus discoidalis. I. Kinematics*," J. Comparative Physiol. A, Neuroethol. Sensory Neural Behav. Physiol., Vol. 188, pp. 39–53, Feb. 2002.

19. Y.-C. Chou, W.-S. Yu, K.-J. Huang, and P.-C. Lin, "*Bio-inspired stepclimbing in a hexapod robot*," Bioinspiration Biomimetics, vol. 7, 036008, pp. 1–19, 2012.

20. J. C. Spagna,D. I.Goldman, P. Lin,D. E.Koditschek, and R. J. Full, "*Distributed mechanical feedback in arthropods and robots simplifies control of rapid running on challenging terrain*," Bioinspiration Biomimetics, Vol. 2, pp. 9–18, 2007.

21. M. Lasa and M. Buehler, "*Dynamic compliant quadruped walking*," in Proc. IEEE Int. Conf. Robot. Autom., 2001, pp. 3153–3158.

22. G. Gabrielli and T. H. von Karman, "*What price speed*?" ASME Mech. Eng., Vol. 72, pp. 775–781, 1950.

23. P. Gregorio,M. Ahmadi, andM. Buehler, "*Design, control, and energetics of an electrically actuated legged robot*," IEEE Trans. Syst., Man, Cybern. B, Cybern., Vol. 27, No. 4, pp. 626–634, Aug. 1997.